Materials Science Forum Vol. 509 (March 2006) pp. 177-186
online at http://www.scientific.net

Time-Dependent Rheological Behavior of Liquid Crystalline Dispersions

J. I. Escalante[1,¥], J. F. A. Soltero[1], F. Bautista[2], J. E. Puig[1] and O. Manero[3]

[1] Departamento de Ingeniería Química (y Física[2]), Universidad de Guadalajara, Blvd. M. G. Barragan 1451, Guadalajara, Jalisco, 44430 – México

[3] Instituto de Investigaciones en Materiales, UNAM, Apdo. Postal 70-360, México, D.F. – 04510

e-mail: ¥jescalante@cucei.udg.mx

Keywords: Rheology, liquid crystalline dispersions, phase-transitions.

Abstract. The rheological response of Aerosol OT (AOT)/water liquid crystalline dispersions is reported here using shear flows. The dispersions exhibit an apparent yield stress and strong non-Newtonian behavior. Steady state and pre-shear dynamical experiments reveal shear-induced structural changes. Under increasing-and-decreasing shear stress experiments, the dispersions exhibit anti-thixotropic hysteresis loops. Once a critical stress is surpassed, an additional thixotropic loop is observed at high shear stress levels. This inverse loop at high shear stresses depends on the previous shear history and on both the rate of change and the maximum attained value of shear stress. The number density of the globular structures in the sheared sample is larger than in one non-sheared sample, but their sizes are smaller than those of the non-sheared sample.

Introduction

The rheology of surfactant-based lamellar liquid crystals has been examined intensively during the past decade [1-9]. In particular, the rheological response to steady state and oscillatory shear flows of lamellar liquid crystals consisting of AOT was studied in detail [4-6, 9]. At concentrations between 1.4 and 18.5 ± 1 wt. %, AOT forms in water biphasic dispersions of lamellar liquid crystals [10]. At around 8.5 wt. %, these dispersions undergo a phase inversion from being water-continuous (microscopic liquid crystallites dispersed in a saturated surfactant aqueous solution) to being liquid crystalline continuous [11]. Below the phase inversion composition, the formation of shear-induced microstructures at high shear rates causes shear-thickening [4]. Upon decreasing shear rates, the dispersion still preserves much of its structure and consequently its high viscosity remains. This behavior is referred to as rheopexy or anti-thixotropy [12, 13]. Above the phase-inversion concentration, the dispersions are strongly non-Newtonian and viscoelastic [4, 9].

According to some observations of thixotropy, this phenomenon always presupposes some molecular or microscopic process by which the structure is modified [12]. In surfactants and in colloidal dispersions, this process is determined by the interaction forces between domains (attractive and electrostatic or steric repulsion forces) coupled with the relative orientation of the domains induced by the flow [14]. The interplay of all the external forces that act on the liquid crystals sometimes produces complicated responses. For instance, the reduction in size of the associated structural units corresponds to smaller resistance against flow, which results in lower viscosities. On the other hand, the orientation of these units by flow can promote increasing interactions that could be attractive, inducing the formation of associating links and agglomeration, resulting in higher viscosities [12].

In this work, the rheological response of lamellar liquid crystalline dispersions of AOT in water under shear flows is examined in detail using controlled-stress rheometry. The changes in the microstructure of the sample are evidenced by polarized light microscopy. Particular attention is given to the hysteresis detected when the samples are sheared under exponentially increasing-and-decreasing shear stress cycles. The presence of an apparent yield stresses and a "critical" stress (τ_c)

that signals the thixotropic-antithixotropic transition are discussed and related with phase changes in these dispersions.

Experimental Section

Sodium bis-(2-ethylhexylsulfosuccinate) or AOT from Fluka had a purity higher than 98 %. Samples were prepared by adding water to 8 % wt dried AOT, then it was homogenized and allowed to equilibrate for at least 7 days at 25 ± 0.1 °C.

Rheological measurements were taken at 25 °C with a Carri-Med CLS-50 controlled-stress rheometer with cone-and-plate geometry (4 cm and 0.035 rad). Steady state shear rate measurements were taken with a Rheometrics RDS II mechanical spectrometer (controlled–strain rheometer) and a cone-and-plate geometry (5 cm and 0.1 rad). Since the domain structure of AOT-based liquid crystalline phases is quite sensitive to shear deformation history, samples were carefully loaded on the plate with a spatula and then the cone was slowly lowered. To prevent changes in composition during measurements for water evaporation, a humidification chamber was placed around the cone and plate fixture. Exponentially increasing-and-decreasing shear stress cycles were performed in the controlled-stress rheometer to determine the degree of thixotropy exhibited by the dispersions. In these experiments, the stress is increased exponentially at time t = 0 from a present value (τ_0 = 0.06 Pa for the rheometer employed) to a prescribed maximum stress (τ_f) at t = t_1. Then, τ_f can be kept constant for a given period of time or the stress can be decreased immediately at the same rate to the initial stress value. Also, two or more consecutive cycles can be performed in the sample with or without a rest period between the cycles.

Experimental microscopy studies were performed at room temperature with a Meopta polarizing transmission microscope.

Results

Figure 1 shows the stress growth upon inception of shear flow, as a function of the applied shear rate upon inception of shear flow for an 8 % AOT dispersion. At low shear rates (curve a, b), stress (τ) increases to a plateau value in times ranging from 200 to 1000 seconds; however, after a few minutes, the stress diminishes and then it grows again to the "true" steady value. Notice that this steady value is reached for times longer than 6000 seconds. At intermediate shear rates (curve c), stress goes through a local maximum, then it decreases and increases again up to the steady state. At higher shear rates (curves d, e and f), stress grows to the steady state after passing through a shallow local maximum or shoulder (inset of fig. 1). This shoulder, which indicates a non-monotonic change in the relationship of τ versus $\dot{\gamma}$, has been reported for cationic surfactants/water gels [7].

Figure 2 shows the steady shear viscosity (η) as a function of $\dot{\gamma}$. The induction time (t_{ind}) defined here as the time at which stress begins to increase before the true steady state, is also shown in this figure. Three regions can be distinguished in the plot of η versus $\dot{\gamma}$. At low shear rates, a shear thinning behavior is observed with long induction times (region I). At intermediate shear rates, a shear thickening behavior is detected and the induction time drops several folds (region II). At high shear rates, a shear-thinning behavior is recovered but the induction times are much smaller. We previously reported this behavior with the same system [4]. However, the levels of viscosity are different, even though the shape of the data is similar, because not enough time was allowed in our previous measurements to reach the true steady state.

Figure 3 depicts stress relaxation after interruption of shear flow as a function of $\dot{\gamma}$ and of the time of application of the shear rate. The inset in each of the figures indicates the times at which the shear flow was interrupted (t_{int}). Shear stress relaxation curves were shifted vertically by an arbitrary factor in order for the relaxation curves to start from the same value. At low shear rates (region I),

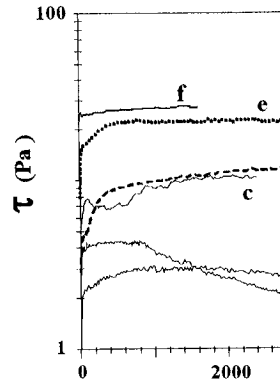

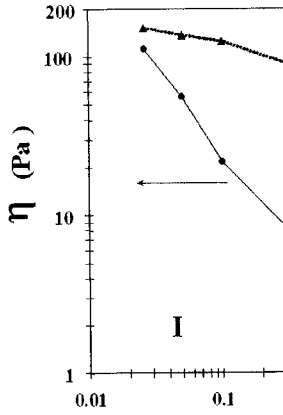

the relaxation follows a sc
the relaxation curves nea
intermediate shear rates (
(Fig. 3B). When this ratio
(curves a and b in Fig. 3B
but finite levels of stress
achieved, which means tha
behavior is seen at high sh
and the level of equilibri
However, at very large va
and e in Fig. 3C) which c
observed in thixotropic ma

Figure 4 reports the i
oscillatory measurements
for times larger than the i
that measured immediate

ssed and related with phase changes in

ka had a purity higher than 98 %. AOT, then it was homogenized and

Carri-Med CLS-50 controlled-stress Steady state shear rate measurements *r (controlled–strain rheometer) and a* ain structure of AOT-based liquid y, samples were carefully loaded on To prevent changes in composition hamber was placed around the cone stress cycles were performed in the py exhibited by the dispersions. In = 0 from a present value ($\tau_0 = 0.06$ ss (τ_f) at $t = t_1$. Then, τ_f can be kept d immediately at the same rate to the be performed in the sample with or

mperature with a Meopta polarizing

, as a function of the applied shear t low shear rates (curve a, b), stress 000 seconds; however, after a few true" steady value. Notice that this intermediate shear rates (curve c), ases again up to the steady state. At state after passing through a shallow h indicates a non-monotonic change urfactants/water gels [7].

$\dot{\gamma}$. The induction time (t_{ind}) defined e steady state, is also shown in this sus $\dot{\gamma}$. At low shear rates, a shear n I). At intermediate shear rates, a ps several folds (region II). At high uction times are much smaller. We owever, the levels of viscosity are ot enough time was allowed in our

flow as a function of $\dot{\gamma}$ and of the ures indicates the times at which the ere shifted vertically by an arbitrary alue. At low shear rates (region I),

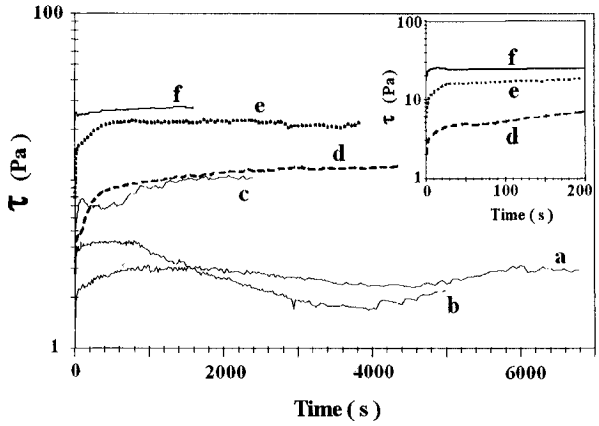

Figure 1. Stress growth after inception of flow for an 8 % AOT dispersion as a function of shear rates (in s^{-1}): (a) 0.026; (b) 0.1; (c) 1.0; (d) 2.0; (e) 10.0; (f) 15.0. Inset: expanded scale for curves d to f.

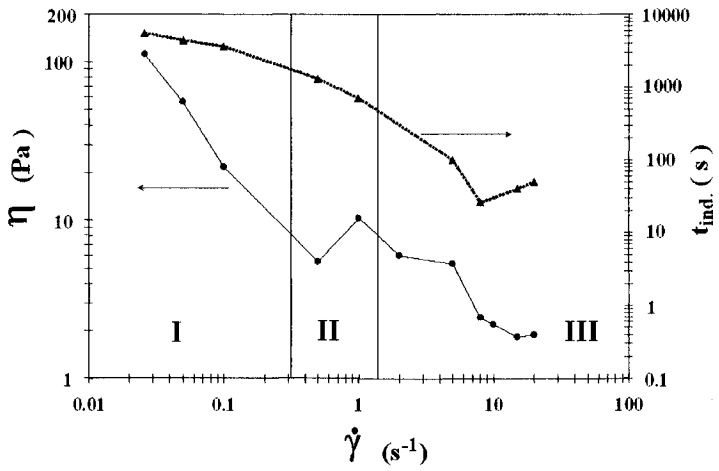

Figure 2. Shear viscosity (η) and induction time (t_{ind}) versus shear rate ($\dot{\gamma}$). Vertical lines indicated the approximated boundaries between regions I, II and III.

the relaxation follows a solid viscoelastic behavior with similar decay times (Fig. 3A). Moreover, the relaxation curves nearly overlap regardless of time at which the flow was interrupted. At intermediate shear rates (region II), two behaviors are observed depending on the ratio of t_{int}/t_{ind} (Fig. 3B). When this ratio is less than one, the relaxation is similar to that observed in region I (curves a and b in Fig. 3B). However, when t_{int}/t_{ind} is higher than one, the sample relaxes to lower but finite levels of stress (curves c and d in Fig. 3B). However, complete relaxation is never achieved, which means that a solid viscoelastic behavior dominates. A more complicated relaxation behavior is seen at high shear rates (region III). At low values of t_{int}/t_{ind} the relaxation time is faster and the level of equilibrium stress is smaller as t_{int}/t_{ind} increases (curves a, b and c in Fig. 3C). However, at very large values of t_{int}/t_{ind}, relaxation is fast and it goes through a minimum (curves d and e in Fig. 3C) which can be very deep (curve e) and then it rises again. This behavior has been observed in thixotropic materials [15].

Figure 4 reports the instantaneous and the infinite-time elastic plateau moduli obtained by oscillatory measurements at 80 s^{-1} as a function of time after subjecting dispersions to a shear rate for times larger than the induction time (see Fig. 2). Here, the instantaneous elastic modulus, G'_0 is that measured immediately after the pre-shear flow has been stopped whereas the infinite-time

elastic modulus, G'_{∞}, represents the value at long times. Also, for comparison, the elastic modulus of a non pre-sheared sample is included (G' = 17.5 Pa). When the pre-shear rate is within region I, G'_{∞} is slightly larger than G'_0 and equal to G'. But, when the pre-shear rate is within region II, $G'_{\infty} \sim G'_0$ but smaller than G'. Finally, when the pre-shear rate is at levels of region III, $G'_{\infty} < G'_0$ but both are larger than G'.

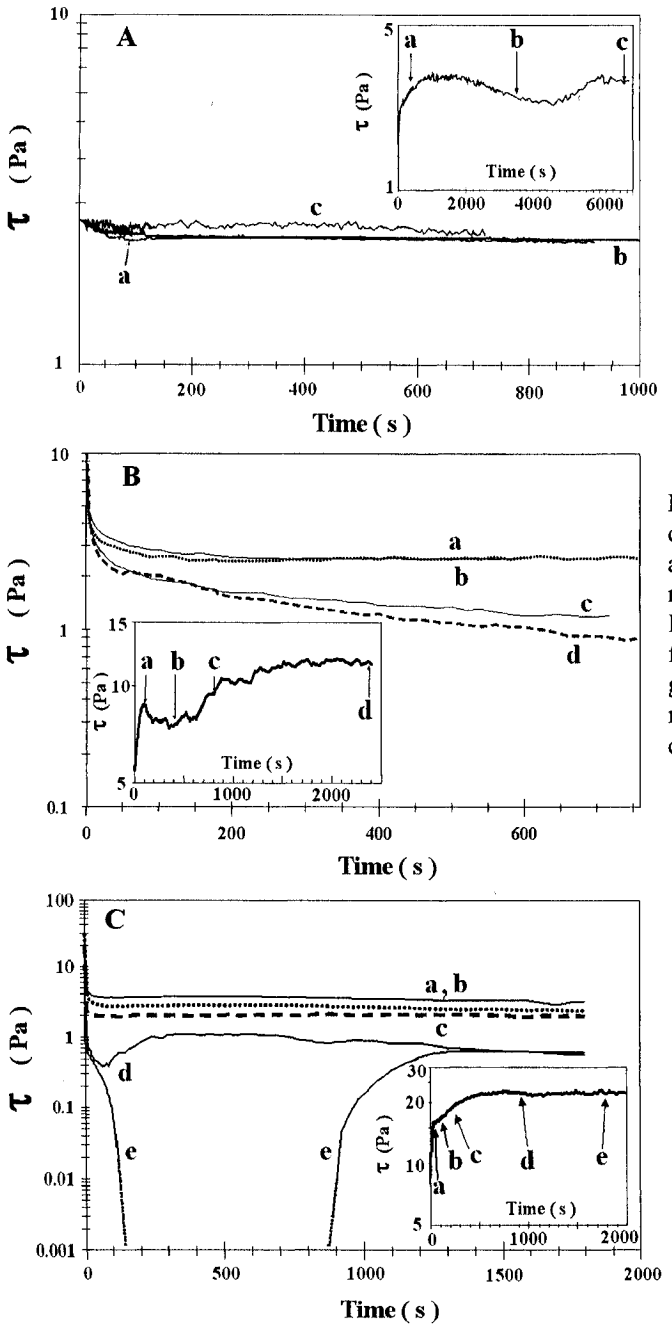

Figure 3. Stress relaxation after cessation of shear flow interrupted at different times in region I (A) and region II (B); and region III (C). Insets depict the times at which the flow was interrupted along the stress growth curve for stress relaxation measurements. Letters in inset corresponds to those in figure.

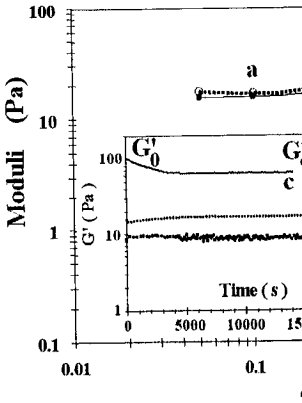

Figure 5 and 6 shows th
where the stress is increased
and then it is decreased to
viscosity as a function of ti
Fig. 5), a large anti-thixotro
flow until a shear stress of
When a second cycle is a
diminishes substantially. It
implies that after the structu
induced-structure also has a
of 3.5 Pa (Fig. 5). Meanwhi
are the existence of a yield
thixotropy to thixotropy b
apparent yield stress is thr
but the value of the critical
which is much larger than th

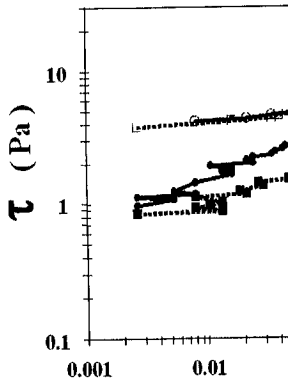

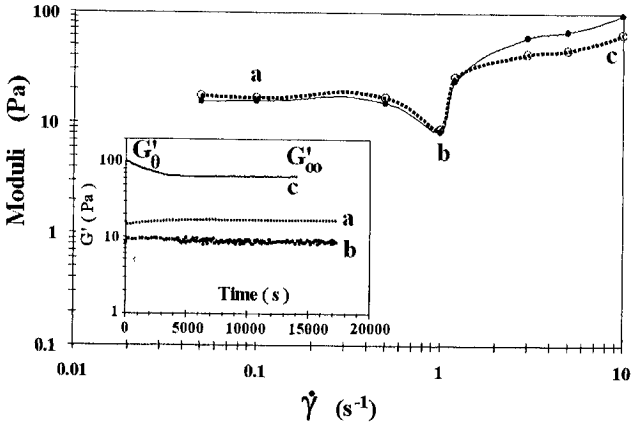

Figure 4. Elastic modulus measured after a pre-shear treatment was applied for times longer than the induction time, as a function of the pre-shear rate: (●) instantaneous modulus and (○) long-time modulus.

Figure 5 and 6 shows the response of a lamellar dispersion to shear stress consecutive cycles where the stress is increased exponentially from 0.06 to 20 Pa and to 50 Pa, respectively, in 120 s, and then it is decreased to the initial value at the same rate. The type of applied cycle and the viscosity as a function of time are depicted in the inset. After the application of the first cycle (in Fig. 5), a large anti-thixotropic hysteresis loop is detected. Also, notice that the dispersion does not flow until a shear stress of 0.7 Pa is exceeded, which means that there is an apparent yield stress. When a second cycle is applied to the same sample, the enclosed area of the hysteresis loop diminishes substantially. It is noteworthy that the returning path is the same in both cycles, which implies that after the structure induced by the first stress cycle is preserved in the second cycle. This induced-structure also has a larger *apparent* yield stress inasmuch as the flow stops at a shear stress of 3.5 Pa (Fig. 5). Meanwhile in Figure 6, the main features after the application of the first cycle are the existence of a yield stress and of a critical stress (τ_c) which signals a transition from anti-thixotropy to thixotropy behavior. Upon application of a second consecutive cycle, the initial *apparent* yield stress is three-fold larger and both the anti-thixotropic and thixotropic loops close but the value of the critical stress remains invariant. Again, there is a final *apparent* yield stress, which is much larger than the initial one.

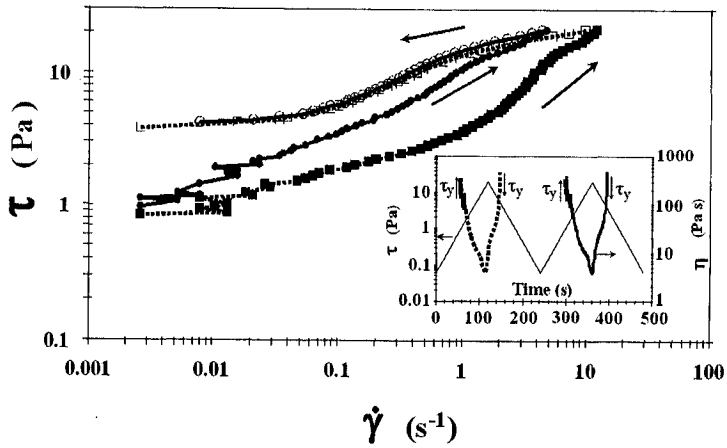

Figure 5. Response of an AOT dispersion to consecutive increasing-and-decreasing stress cycles. Full symbols indicated the increasing stress mode whereas open symbols denote the decreesing stress mode. (■, □) First cycle; (●,○) second cycle. Inset: applied stress program (from 0.06 to 20 Pa in two minutes) and viscosity versus time.

The effect of maintaining the maximum applied shear stress for a certain period of time is shown in Fig. 7 and 8 for two levels of final shear stress. In Figure 7, the maximum stress is smaller than

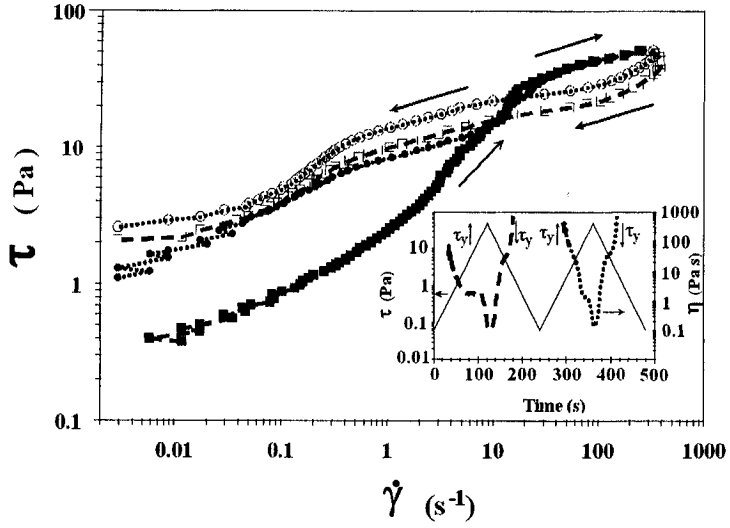

Figure 6. Time-varying programs of shear stress applied. Full symbols indicated the increasing stress mode whereas open symbols denote the decreasing stress mode. (■, □) First cycle; (●,○) second cycle. Inset: applied stress program (from 0.06 to 50 Pa in two minutes) and viscosity versus time.

the τ_c whereas in Figure 8, the maximum applied stress is larger than τ_c. Inset *a* in these figures de picts the type of stress program applied and the viscosity as a function of time. Inset *b* in these figures shows the shear rate as a function of time during which the maximum shear stress was maintained. When the maximum applied stress is smaller than the critical value, an anti-thixotropic loop is observed (Fig. 7). The response of the sample when the maximum stress is maintained, however, is characteristic of an anti-thixotropic material: during the time that the stress is maintained constant, the shear rate decreases, that is, the sample tries to slow down at constant stress (inset *b* in Fig. 7). However, in the cycle where the maximum applied stress exceeds the τ_c, an inversion of the hysteresis loop is observed (Fig. 8), similar to the one shown in Fig. 6. However, when the applied shear stress is maintained at this level, the shear rate first increases and then decreases. This behavior is typical of a thixotropic material.

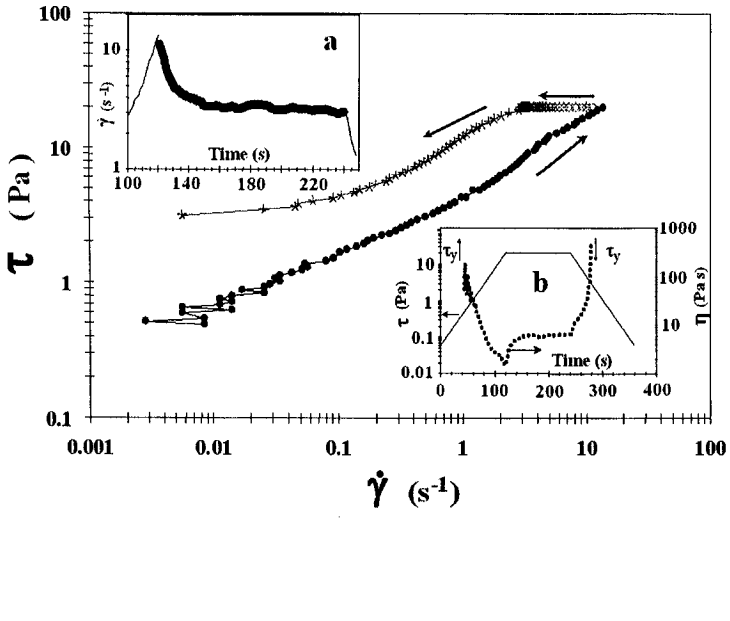

Figure 7. Response to single in-creasing-and-decreasing stress cycle, where the maximum applied stress (at a level below the critical stress) was maintained constant for a certain amount of time. Inset (a): Applied stress program (0.06 to 20 Pa) and viscosity as a function of time. Inset (b): Shear rate versus time during the period of time when the maximum stress is maintained constant.

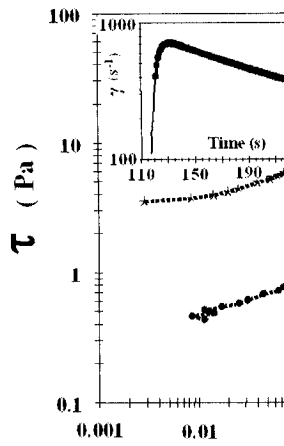

Figure 9 depicts photo
microscope after being sub
series of photographs corre
clearly seen, which are typ
texture, size and number d
sample not subjected to sh
number density of the Malt

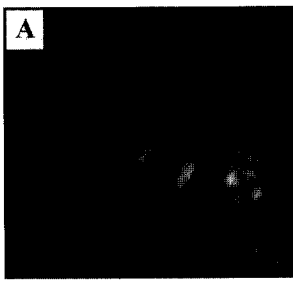

Figure 9. Photographs ta
subjected to differe

Discussion and Conclusio

Induced-structures and st
documented in surfactant-
induced microstructures a
microstructures may be lo
more complicated and the

Liquid crystalline dispe
that very long times may
state depends on the level
show below, the structural
and the complex rheologic

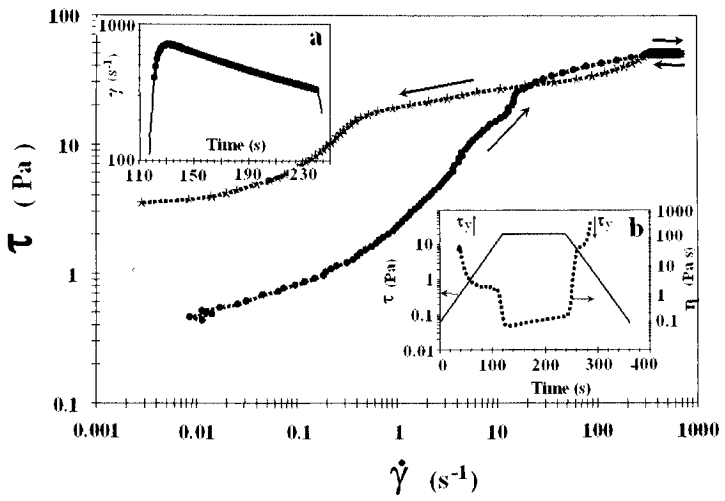

Figure 8. Response to single increasing-and-decreasing stress cycle, where the maximum applied stress (at a level above the critical stress) was maintained constant for a certain amount of time. Inset (a): Applied stress program (0.06 to 50 Pa) and viscosity as a function of time. Inset (b): Shear rate versus time during the period of time when the maximum stress is maintained constant.

Figure 9 depicts photographs of the samples taken through cross polarizers in an optical microscope after being subjected to the stress cycles. The levels of the applied shear rates in these series of photographs correspond to regions I, II and III. In these photographs, Maltese crosses are clearly seen, which are typical in lamellar liquid crystalline dispersions [16]. At low shear rates, the texture, size and number density of the spherulites of the sample (Fig. 9A) are similar to those of a sample not subjected to shear flow. However, it is evident that as the shear rate is increased, the number density of the Maltese crosses increases whereas their sizes decrease (Figs. 9B and 9C).

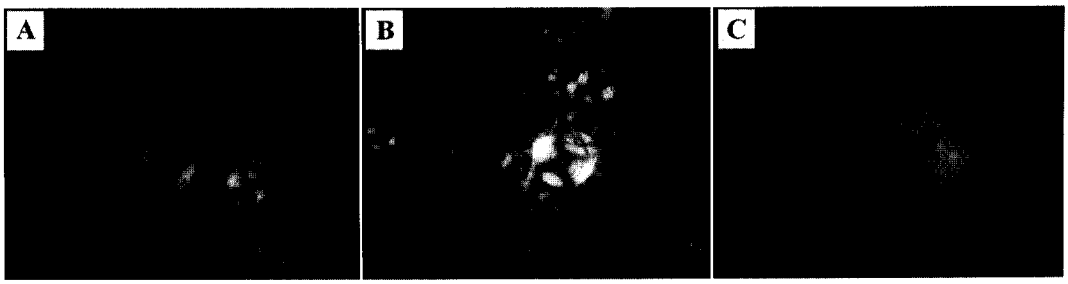

Figure 9. Photographs taken by light microscopy under cross polarizers of AOT dispersions subjected to different levels of shear stress: (A) region I; (B) region II; (C) region III.

Discussion and Conclusions

Induced-structures and structural changes caused by shear and extensional flows have been documented in surfactant-based systems. In very labile systems, such as micellar solutions, the induced microstructures are short-lived [17-20]. However, in liquid crystalline systems, induced microstructures may be long-lived [21-23]. In this situation, the rheological behavior becomes even more complicated and the reported flow properties may not correspond to the *true* steady values.

Liquid crystalline dispersions of AOT depict this kind of behavior. Figure 1 clearly demonstrates that very long times may be needed to achieve steady values. The time required to reach steady state depends on the level of applied shear rate (Fig. 2) and surfactant concentration. As we will show below, the structural changes induced by the shear flow are responsible for the long transients and the complex rheological behavior.

Depending of the level of applied shear rate (or shear stress), three different regions are detected (Fig. 2). We first reported this type of viscosity versus shear rate curve in the same system, but measurements were not taken for times long enough to reach the true steady state and so, viscosity values reported earlier are several folds smaller [4]. This unusual behavior was detected within the whole biphasic liquid crystalline dispersion region [4]. More recently, Escalante and Hoffmann [23] reported a similar rheological behavior and attributed it to a lamellar-to-vesicle transition.

At low shear rates (region I), long transients after inception of shear flow (Fig. 1) and a shear thinning behavior in steady shear (Fig. 2) are observed. Also, stress after cessation of shear flow is typical of a solid viscoelastic material and does not appear to be dependent on the time of interruption of flow (Fig. 3A). Notice that the instantaneous (G'_0) and the long-time modulus (G'_∞) are similar and equal the elastic modulus measured in a non pre-sheared sample (Fig. 4). More importantly, the texture and number density and size of the spherulites are similar to those of an unperturbed sample (Fig. 9A). The implication is that at low levels of shear rate, the original structure is preserved, or at least, it is not modified substantially. Nevertheless, it is significant that long times are required to reach steady state.

At intermediate shear rates (Region II), a shear thickening behavior is detected with shorter transients. However, when the sample is sheared for times longer than the induction time and the relaxation is followed after cessation of slow, a different behavior is noticed (Fig. 3B). Moreover, the elastic modulus of a non pre-sheared sample is larger compared to either G'_0 or G'_∞ (Fig. 4). Polarizing light microscopy reveals a finer structure than that of the non-sheared one (cf. Figs. 9A and 9B).

More complicated behavior is observed when the dispersions are sheared at shear rate levels of region III. Transients are much shorter than in regions I and II, and shear thinning behavior is recovered (Fig. 2). Stress relaxation after cessation of shear flow depicts a complex nature. When the flow is stopped at times shorter than t_{ind}, a solid viscoelastic behavior is observed and the sample maintains high levels of stress, just like in regions I and II (cf. Fig. 3C with Figs. 3B). However, when the flow is stopped after long times, a minimum in the stress relaxation curve is seen, which can be very pronounced (curve e in Fig. 3C). Moreover, the long time and the instantaneous moduli differ substantially from each other, and both are much larger than that of the non pre-sheared sample, indicating substantial changes in microstructure. Polarizing light microscopy (Fig. 9C) corroborates these changes.

Thixotropic or anti-thixotropic behavior is evident by observing the response under consecutive increasing-and-decreasing shear stress cycles. In this case, the increasing and the decreasing shear stress curves do not coincide, which results in a hysteresis loop. However, it is well known that repetition of time-varying programs of shear stress reduces the hysteresis until finally an equilibrium curve is obtained devoid of thixotropic effects [12].

The time-varying programs of shear stress applied here yield an anti-thixotropic response as long as a critical stress is not surpassed (Figs. 5 and 7). The extension of the hysteresis loops decreases after consecutive cycles are applied to the sample, just as described by Mewis [12]. Nevertheless, the downward paths in the first, second and consecutive cycles coincide, in spite that the upward paths may be different (Figs. 5 and 6). Evidently, these results suggest structural changes induced by exponential shear flow. Photographs taken on dispersions subjected to different levels of shear stress in one of these exponentially increasing-and-decreasing stress programs confirms this hypothesis (Fig. 9). It is noteworthy that steady shear experiments also demonstrate that these dispersions exhibit anti-thixotropy, inasmuch as the stress (or viscosity) raises with time when they are subjected to a constant shear rate (Fig. 2). Incidentally, anti-thixotropy has been found mostly in dispersions and concentrated suspensions [24, 25] but also shear-induced structures have been observed in micellar solutions [26].

To demonstrate that the structural changes induced by flow are long-lived, stress cycles were

performed leaving a rest pe
same path is followed in th
rest period [13].

On the other hand, once
thixotropic loop (Figs. 6 an
the rate of change and the n
another change in the numb
presence of an inverse hyst
that the characteristic tim
corresponding to the recipro

In summary, we have pr
dispersions of AOT. These
shear flow

Acknowledgement

This work was supported b
Guadalajara for funds to im

References

[1] P. Oswald and M. Allai

[2] T. Matsumoto, T. Heiuc

[3] S. Paasch, F. Schambil

[4] M. Valdés, O. Manero,
p. 59.

[5] O. Robles-Vásquez, S.
O. Manero: J. Colloid I

[6] J. F. A. Soltero, O. Rob

[7] A. Goldzal, A. M. Jami
Vol. 180 (1996), p. 261

[8] J. F. A. Soltero, F. Bau
J. Colloid Polym. Sci.

[9] K.W. McKay, W.G. M
p. 37.

[10] E. I. Franses and T. J.

[11] A.H. Alexopoulos, J.
p. 26.

[12] J. Mewis: J.. Non-Ne

[13] J. F. A. Soltero: PhD

[14] W. B. Russel, D. A. S
University Press, Ne

[15] W. H. Bauer and E. A
(Academic Press, Ne

performed leaving a rest period up to one hour between cycles (not shown). Results show that the same path is followed in the second cycle, regardless of whether is immediately applied or after a rest period [13].

On the other hand, once a critical shear stress is reached, the anti-thixotropic loop reverses into a thixotropic loop (Figs. 6 and 8). This inverse loop depends on the previous shear history and both the rate of change and the maximum value of shear stress [6]. Again, polarizing microscopy shows another change in the number density and size of the liquid crystalline microdomains (Fig. 9C). The presence of an inverse hysteresis loop at high stress levels, in this case, a thixotropic loop, means that the characteristic time associated with the recovery of the structure is larger than that corresponding to the reciprocal of the applied shear rate.

In summary, we have presented the complex rheological behavior of aqueous liquid crystalline dispersions of AOT. These complex responses are related to microstructural changes induced by shear flow

Acknowledgement

This work was supported by CONACyT (grant # 3343P-E9607). We are grateful to the University of Guadalajara for funds to import the controlled stress rheometer.

References

[1] P. Oswald and M. Allain: J.. Colloid Interface Sci, Vol. 126 (1988), p. 45.

[2] T. Matsumoto, T. Heiuchi and K. Horie: Colloid Polym.. Sci.. Vol. 267 (1989), p. 71.

[3] S. Paasch, F. Schambil and M. Schwuger: Langmuir Vol. 5 (1989), p. 1344.

[4] M. Valdés, O. Manero, J. F. A. Soltero and J. E. Puig: J. Colloid Interface Sci. Vol. 160 (1993), p. 59.

[5] O. Robles-Vásquez, S. Corona-Galván, J. F. A. Soltero, J. E. Puig, S. Tripodi, E. Vallés and O. Manero: J. Colloid Interface Sci. Vol. 160 (1993), p. 65.

[6] J. F. A. Soltero, O. Robles-Vásquez, J. E. Puig and O. Manero: J. Rheol. Vol. 39 (1995), p. 235.

[7] A. Goldzal, A. M. Jamieson, A. J. Mann, J. Polar and Ch. Rosenblatt: J. Colloid Interface Sci.. Vol. 180 (1996), p. 261.

[8] J. F. A. Soltero, F. Bautista, E. Pecina, J. E. Puig, O. Manero, Z. Proverbio and P. C. Schulz: J. Colloid Polym. Sci. Vol. 78 (2000), p. 37.

[9] K.W. McKay, W.G. Miller, J.E. Puig and E.I. Franses: J. Dispersion Sci. Tech. Vol. 12 (1991), p. 37.

[10] E. I. Franses and T. J. Hart: J. Colloid Interface Sci. Vol. 94 (1983), p. 1.

[11] A.H. Alexopoulos, J. E. Puig and E. I. Franses: J.. Colloid Interface Sci.. Vol. 128 (1989), p. 26.

[12] J. Mewis: J.. Non-Newt. Fluid Mech. Vol. 6 (1979), p. 1.

[13] J. F. A. Soltero: PhD Thesis, Universidad Nacional Autónoma de México (1994).

[14] W. B. Russel, D. A. Savile and W. R. Schowalter: *Colloidal Dispersions* (Cambridge University Press, New York 1989).

[15] W. H. Bauer and E. A. Collins: in F. R. Eirich (ed.) *Rheology: Theory and Applications* (Academic Press, New York 1967) p. 423.

[16] F. B. Rosevear: J. Am. Oil Chem. Soc. Vol. 31 (1954), p. 628.

[17] H. Rehage, H. Hoffmann and I. Wunderlich: Ber. Bunsenges Phys. Chem. Vol. 90 (1986), p. 1071.

[18] E. Cappelare, R. Cressely, R. Makhloufi and J. P. Decruppe: Rheol. Acta Vol. 33 (1994), p. 431.

[19] J. Narayanan, E. Mendes and C. Manohar: J. Phys. Chem. Vol. 100 (1996), p. 18524.

[20] E. K. Wheeler, P. Fischer, G. G. Fuller: J. Non.Newtonian Fluid Mech. Vol. 75 (1998), p. 193.

[21] N. Shahidzadeh, D. Bonn, O. Agueerre-Chariol and J. Meunier: Phys. Rev. Lett. Vol. 81(1998), p. 4268.

[22] E. Mendes, J. Narayanan, R. Oda, F. Kern, S. J. Candau and C. Manohar: J. Phys. Chem. B Vol. 101(1997), p. 2256.

[23] J. I. Escalante and H. Hoffmann: J. Phys.: Cond. Matter Vol. 12 (2000), p. A483.

[24] J. B. Llanas and R. N. Gonzalez: Nature Vol. 191 (1961), p. 1384.

[25] Dc. H. Cheng: J. Phys. D: Appl. Phys. Vol. 7 (1984), p. L155.

[26] I. Wunderlich, H. Hoffmann and H. Rehage: Rheol. Acta Vol. 26 (1987), p. 532.

Materials Science Forum Vol. 509
online at http://www.scientific.net

Preparation of Size

C. A. Cortés Escol

[1]Centro de Investigació
Norponi

[2]Escuela Superior de Ing
López Mate

[a]j

Keywords: Sol-gel, Monoc

Abstract. In this work, w
(SBF) procedure for the pr
of size and controlled dia
precursor molecule and hy
bonds are carried out. Th
hydroxide solution as amn
are presented (reaction yie
are discussed. This proced
preparation process. As a r
of 250 to 850 nm is that of
contents in the range of 8 -

Introduction

Precious opal, which is a
of uniform size spheres ar
of atoms in a crystal, but i
that produces the play of
between the spheres and t
the interstices [7, 8]. Fu
precious opal highly order
assemble monodisperse si
10 months to get a green
wavelengths only and ar
optoelectronic materials [
photonic crystals for the
Spherical and monodisper
microscope analysis equip

The first step for the
controlled size and a unif
technique) [10]. The meth
Gel process in alkaline pH
et al. [10] developed a sili
varying the morphological
reagent.

The hydrolysis and co
the most important precu